❒ 227

Heavy metals removal by thiol modified oak charcoal: adsorption efficiency and selectivity

Zeinab Ezzeddine[1], Batoul Solh[2], Hussein Hamad[3]
[1,3]Department of Chemistry, Faculty of Science, Lebanese University, Lebanon
[2]Platform for Research and Analysis in Environmental Sciences, Lebanese University, Lebanon

Article Info	ABSTRACT
	Herein, the removal of heavy metals on thiol modified oak charcoal was investigated. The modified charcoal was characterized by X-ray diffraction, granulometric analysis, and infrared spectroscopy. Then, its adsorption efficiency for the removal of Cd^{2+}, Cu^{2+}, and Pb^{2+} from water was tested. The effects of several conditions on metals adsorption were investigated such as contact time, pH, electrolytes and the initial metal ions concentration. The adsorption capacities were high (197, 250, and 214 mg g^{-1} for Cd^{2+}, Pb^{2+}, and Cu^{2+} respectively). The selectivity was also dependent on the metal ions nature and the functional group used. The mechanism of adsorption is complex where several types of interaction between metal ions and the adsorbent surface are involved. *This is an open access article under the <u>CC BY-SA</u> license.*
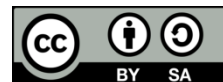
Corresponding Author:

Zeinab Ezzeddine
Department of chemistry
Faculty of Science, Lebanese University
Nabatieh, Lebanon
Email: zeinab.ezzeddine.1@ul.edu.lb

1. INTRODUCTION

Heavy metals are among the most dangerous pollutants discharged into the environment every day. They are persistent in nature and have accumulation tendcy in living organisms [1]. Cu^{2+}, Cd^{2+}, and Pb^{2+} are usually present in wastewater. Although these metals are essential for life in small amounts, the exposure of high levels can lead to serious health problems [2]. Many techniques are available for heavy metals removal from water, but adsorption is attracting a great deal of attention due to its simplicity and versatility [3]. Carbonaceous materials have been widely applied for waste water treatment since they have large surface area and can remove several types of contaminants [4]. Many researchers noted the effectiveness of modified activated carbon (AC) in heavy metals adsorption [5]-[7]. More research on activated carbon is still needed to better understand the performance towards certain contaminants and thus to enhance their removal from of wastewater.

Modifying AC surface by oxidizing agents is a widly used [8], but this technique tends to decrease the surface area of AC [9] so alternative methods were investigated to increase the removal of heavy metals without affecting the carbon structure such as modification with organic ligands [4]. Moreover, investigating the mechanism of adsorption is crucial for the synthesis of selective adsorbents with elevated properties for specific applications in liquid phase. Understanding the mechanism of metal ions binding is essential for describing and predicting the adsorption operation. The function of a specific surface group is important in fabricating novel adsorbents with higher efficiency [10].

In this study, oak charcoal carbon was modified by 3-mercaptopropyl trimethoxysilane (MPTMS). This modification method is practical and inexpensive which favors its applicability. Then the adsorption capacity for Cu^{2+}, Cd^{2+}, and Pb^{2+} removal was studied in details. The effects of several parameters on the process of adsorption were performed, as contact time, solution pH, the electrolyte effect and metal ions concentration. The kinetic data of adsorption experiments were studied by pseudo-first and pseudo-second-order models. The isotherms were fitted by both Freundlich and Langmuir. Moreover, the selectivity was studied as well in a ternary ions mixture.

2. RESEARCH METHOD

2.1. Chemicals

The 3-MPTMS, hydrochloric acid (HCl, 37%), sodium hydroxide (NaOH), toluene and cadmium chloride ($CdCl_2.H_2O$; 93%) were purchased from Sigma Aldrich, while lead nitrate ($Pb(NO_3)_2$ 99.9%) was purchased from UNICHEM. Copper nitrate ($Cu(NO_3)_2.3H_2O$) from Alpha Chemika. All chemical reagents were used as received. Distilled water was produced in the laboratory.

2.2. Activated carbon modification

Commercially available oak charcoal was used (AC). Prior to usage, the carbon was grinded, washed with boiled distilled water and oven-dried at 120 °C for 24 h. Then, 15 ml MPTMS was added to 50 g of AC in 300 ml toluene under magnetic stirring for 16 h at 200 rpm. After filtration, the resulting MPTMS-carbon was washed with 150 ml toluene then dried at 150 °C for 4 h. The obtained carbon was referred to as AC-SH as shown in Figure 1.
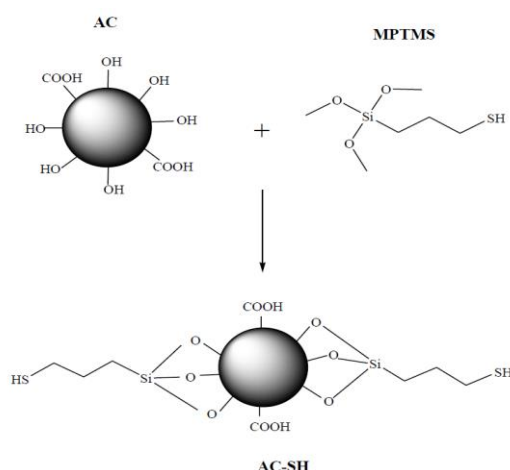

Figure 1. Modification of AC with MPTMS

2.3. AC characterization

The granulometric analysis that determines the size distribution after modification was conducted using Partica LA-950V2 Horiba. After modification, the functional groups were determined by Fourier Transform Infrared (FTIR) Spectroscopy in the range of 4000-400 cm^{-1}. The carbon samples were blended with KBr then pressed into pellets and analyzed with FT-IR-6300 JASCO. X-ray diffraction was performed in the range of 2θ between 10° and 60° on a D8 Bruker diffractometer.

2.4. Batch adsorption tests

Different concentrations of metal ions solutions were prepared salts in distilled water from their corresponding. The solution pH was modified using 0.1 M HCl and 0.1 M NaOH solution. In typical batch studies, 0.1 g of the AC-SH was put in a beaker containing 50 mL of a metal solution of the desired concentration. The beaker was stirred at RT at 300 rpm for 120 min. After finishing each step, the solution was filtered and the metals concentration was detected for each metal using Atomic Adsorption Spectrophotometer (RAYLEIGH WFX-210). The metal ions adsorption percentage was calculated by (1) [11].

$$R = \frac{C_0 - C_t}{C_0} \times 100 \qquad (1)$$

Where R is the adsorption rate (%), C_0 is the initial concentration and C_t is the concentration at time t. The adsorption capacity of the adsorbent at equilibrium was calculated by (2).

$$q_e = \frac{(C_0 - C_e)V}{m} \qquad (2)$$

Where qe is the equilibrium adsorption capacity in mg g^{-1}, C_0 is the initial concentration and C_e is the concentration at equilibrium, V is the volume in L of metal solution and m is the mass in g of the adsorbent. For obtaining the isotherms, the batch experiments the initial metal ions concentrations were altered between 10 mg L^{-1} and 500 mg L^{-1}. The solutions were then filtered by a 0.45 μm syringe filter and the remaining metal ions were measured by AAS in order to calculate C_e and q_e.

3.   RESULTS AND DISCUSSION
3.1. X-ray diffraction analysis and granulometric analysis
Figure 2(a) shows the diffractograms of the activated carbon samples before and after MPTMS modification. As shown in the figure, the backbone of the AC was not affected by modification thus the structure was not altered by organic ligands anchoring. The size distribution of AC samples after modification are presented in Figure 2(b) a homogenous main particle distribution population was obtained with average diameter 19 µm.
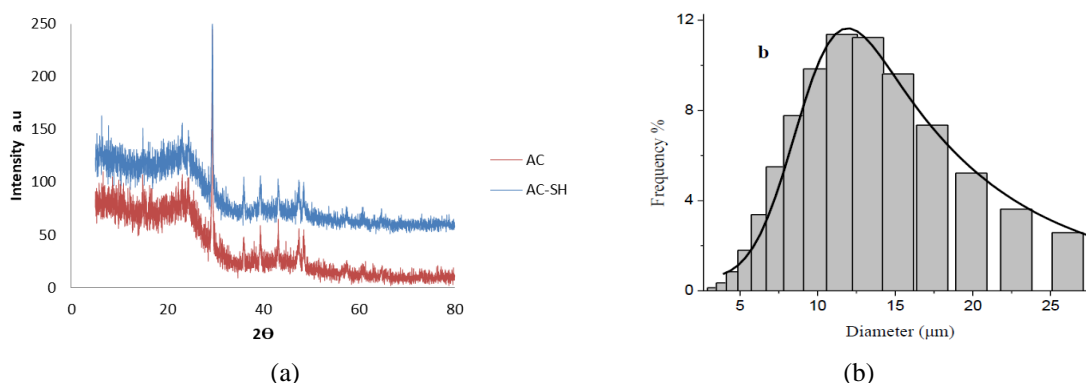

Figure 2. X-ray and granulometric analysis, (a) X-ray diffraction analysis of AC and AC-SH, (b) granulometric analysis of AC-SH

3.2. FT-IR spectroscopy
The modification of the AC surface was analyzed by FT-IR spectroscopy. The S–H functional group frequencies were detected as shown in Figure 3. The broad band in the region 3300-3600 cm^{-1} in the AC and AC-SH spectra, is typically related to –OH stretching while the bands at 1439 cm^{-1} and 1750 cm^{-1} are characteristics of –COOH group. The peak at 2550 cm^{-1} correspondsto the thiol group [12]. The weak peaks at 2971 cm^{-1} and 2865 cm^{-1} belong to the stretching vibrations of –C–H bonds [13]. The strong peak near 1054 cm^{-1} is due to Si–O stretching vibrations [12]. The peaks around 1246 cm^{-1} and 693 cm^{-1} are characteristics of Si-O-C and Si-C respectively.

3.3. The pH effects
Figure 4(a) shows the adsorption capacity of AC-SH as a function of pH which was varied between 2 and 8. At low pH values, adsorption decreased for the three metal ions due to the competition with H_3O^+ ions and the formation of positively charged moieties on the carbon surface (Figure 4(b)). As pH increased, adsorption increased and the maximum removal was reached between pH 5 and 6. At higher pH values, adsorption remained constant for lead and cadmium while it decreased for copper due to the formation of copper precipitate. So, the rest of the experiments were performed at pH=6.
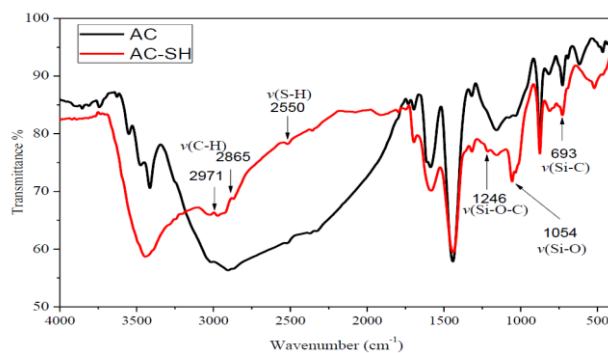
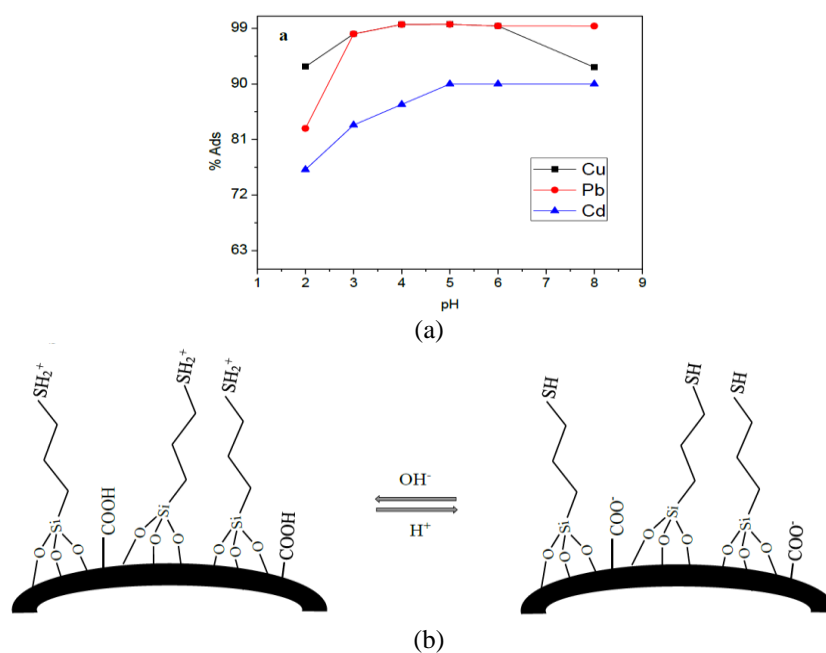Figure 3. FT-IR analysis for carbon before and after modification with MPTMS

(a)

(b)

Figure 4. The pH effect: (a) metal ions adsorption and (b) on AC-SH surface

3.4. Adsorption kinetic models
3.4.1. Pseudo-first order

The pseudo first-order kinetic model is expressed as (3).

$$\frac{dq_t}{dt} = k_1(q_e - q_t) \tag{3}$$

Where qt and qe are the quantity of metal ions adsorbed (mg g^{-1}) at time t (min) and at equilibrium respectively, and k$_1$ is the rate constant of adsorption (min^{-1}). Integrating (3) with the following boundary conditions: t = 0 to t = t and qt = 0 to qt = qt yields (4).

$$\ln (qe-qt) = \ln qe - k_1t \tag{4}$$

The plot of ln (qe - qt) versus t should give a linear relationship where qe and k1 can be calculated from the plot intercept and slope respectively [14].

3.4.2. Pseudo-second order

The pseudo-second-order sorption rate is expressed in (5).

$$\frac{dq_t}{dt} = k_2(q_e - q_t)^2 \tag{5}$$

Where k_2 is the pseudo-second order rate constant (g mg^{-1} min^{-1}), q_t and q_e are the quantity of metal ions adsorbed at t time and at equilibrium (mg g^{-1}) respectively. For the boundary conditions, t = 0 to t = t and q_t = 0 to $q_t = q_t$, the integrated form of (6).

$$\frac{t}{q_t} = \frac{1}{k_2 q_e^2} + \frac{t}{q_e} \tag{6}$$

According to (6), a plot of t/q_t versus t should yield a straight line from which q_e and k_2 can be determined from the slope and intercept of the plot, respectively [15]. Metal ions adsorption as a function of contact time is illustrated in Figure 5(a). The kinetic parameters as well as the experimental equilibrium capacities are listed in Table 1. The obtained results revealed that Cu^{2+}, Cd^{2+}, and Pb^{2+} adsorption on AC-SH followed the pseudo-second order kinetic model (Figure 5(b)). This suggests that the adsorption rate depends mainly on the content of active adsorption site on the adsorbent matrix.
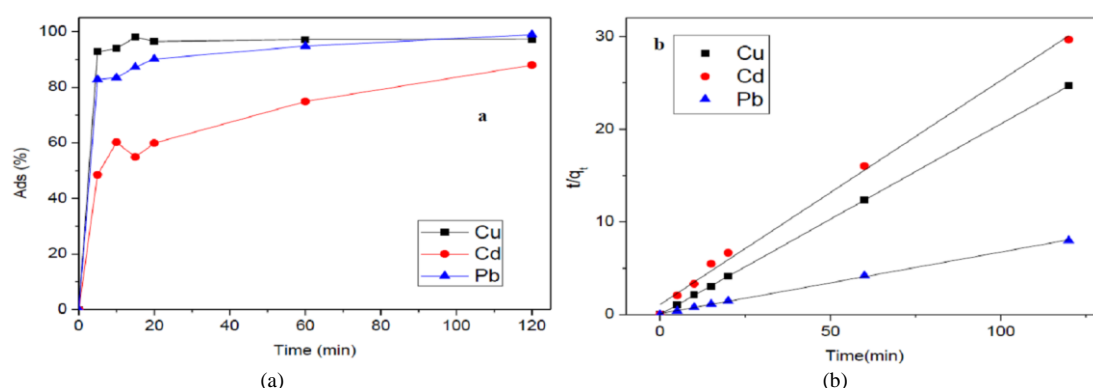

(a)   (b)

Figure 5. Contact time effect on metal ions adsorption: (a) pseudo-second order kinetic model and (b) ([M^{2+}] = 0.14 mmol L-1, pH=6 at RT)

Table 1. parameters of the two kinetic models

	qe^{exp} (mg g^{-1})	First order kinetic model			Second order kinetic model		
		k_1 (min^{-1})	qe^{cal} (mg g^{-1})	R^2	k_2 (g mg^{-1} min^{-1})	qe^{cal} (mg g^{-1})	R^2
Cu^{2+}	4.84	0.017	54	0.357	1.16	4.85	0.999
Pb^{2+}	14.8	0.021	10	0.945	0.039	15	0.999
Cd^{2+}	6.57	0.07	2.5	0.438	1.52	6.62	0.999

3.5. Adsorption Isotherms
3.5.1. Langmuir isotherm model
The model Langmuir Isotherm suggests a monolayer coverage of a finite number of identical sites present on the surface so that no more adsorption occur. Based on these assumptions, Langmuir represented (7) [16].

$$q_e = \frac{K_L \times q_{max} \, C_e}{1 + K_L C_e} \tag{7}$$

Where q_{max} is the maximum adsorption capacity (monolayer coverage), i.e., mg of the adsorbate per (g) of adsorbent and K$_L$ is Langmuir isotherm constant.

3.5.2. Freundlich isotherm model
This model explains a reversible and a non-ideal adsorption, not limited to monolayer formation. This model can be utilized for multilayer adsorption [17]. The equation is expressed as (8).

$$q_e = K_f C_e^{1/n} \tag{8}$$

Where K_f is Freundlich isotherm constant (mmol g^{-1}) and n is the adsorption intensity. The slope is a measure of surface heterogeneity and it ranges between 0 and 1. If n = 1 then the partition between the two phases is independent of the concentration. When the value of n decreases, the adsorbent surface heterogeneity increases. The value gets closer to zero when the system is more heterogeneous.

The obtained results for both models are presented in Figure 6 and their parameters are reported in Table 2. The values of R^2 for Langmuir model for Pb^{2+} were greatest while the R^2 values of Freundlich model for Cu^{2+} and Cd^{2+} were greatest. These obtained results proves that for Pb^{2+}, Langmuir model fitted better while for Cu^{2+} and Cd^{2+} Freundlich model gave a better fit.
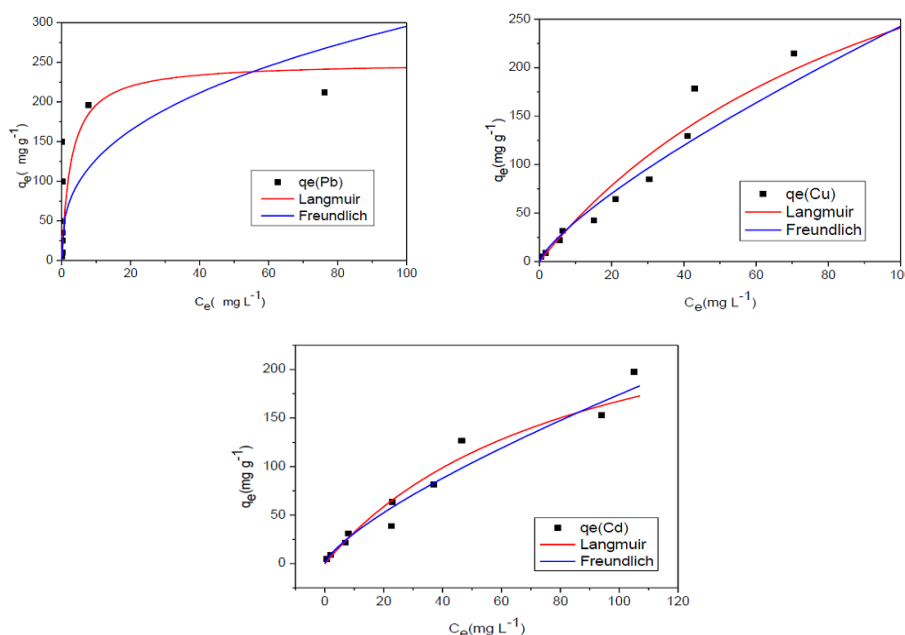

Figure 6. Freundlich and Langmuir models fit for Pb^{2+}, Cu^{2+}, and Cd^{2+} (pH=6 at RT)

Table 2. Comparison of Freundlich and Langmuir models for Me2+ removal by AC-SH

Me^{2+}	q^{exp} (mg g^{-1})	Langmuir model			Freundlich model		
		q^{cal} (mg g^{-1})	K_L (L mg^{-1})	R^2	n	K_f (mg g^{-1})	R^2
Cu^{2+}	214	199	0.01	0.742	1.29	7	0.972
Pb^{2+}	250	242	0.363	0.988	2.73	55	0.339
Cd^{2+}	197	171	0.012	0.578	1.34	5.61	0.979

3.6 Selectivity and effect of electrolytes
3.6.1. Selectivity

There were 0.1 g AC-SH added to 50 ml of ternary ion solution of Pb^{2+}, Cd^{2+}, and Cu^{2+} of equimolar concentration. The sorption decrease in ternary metal ions solution compared to single metal ions may be attributed to the less availability of binding sites (Figure 7(a)). In ternary metal solution, the binding sites are divided competitively among the three ions. It was observed that Pb^{2+} has the highest adsorption capacity over Cu^{2+} and Cd^{2+} with respective rates of 90.9%, 88.6%, and 86%. The adsorption capacity of AC-SH in removing heavy metals from aqueous solution could be arranged in the following order: Pb^{2+}> Cu^{2+}> Cd^{2+}.

In general, the sequence of adsorption capacity of heavy metals is largely dependent on physicochemical properties of metals. Pb^{2+} is preferentially adsorbed over Cu^{2+} and Cd^{2+} onto the binding sites of the AC-SH surface due to its high electronegativity (2.33) compared to that of Cu^{2+} and Cd^{2+} (1.9 and 1.69 respectively). Moreover, thiol modified adsorbents were found to be more selective for Pb^{2+} more than other metal ions [18].

3.6.2. Effect of electrolytes

Generally speaking, the adsorption rate of the metal ion slightly decreases after changing the matrix electrolyte type. In the presence of NaCl, the metal ions adsorption on AC-SH decreased by 1%, 0.8% and 2.27% for Pb^{2+}, Cd^{2+} and Cu^{2+} respectively. On the other hand, the presence of KCl affected the adsorption rate by 1.6% and 5.7% for Pb^{2+} and Cd^{2+} respectively while the removal of Cu (II) has not been affected (Figure 7(b)). This decrease is due to the fact that the existence of NaCl or KCl results in complexation of chloride and competition of sodium and potassium ions, with the metal ion to occupy some specific sites of the modified AC. This observation may be related to the formation of various complexes of metal ions with Cl^- ligands (like $CdCl_2$, $CdCl_3^-$, $PbCl_4^2$, etc.) where the Cl^- ion may coordinate with metal ions and be treated as an inner sphere complex with the surface. Furthermore, the adsorption rate of the three studied metal ions in decreasing order: $Cu^{2+} > Pb^{2+} > Cd^{2+}$ and this is linked directly to the affinity of the adsorbent towards each metal ion, the adsorption mechanism and the characteristics of each metal ion. AC-SH has lesser affinity towards Cd^{2+} that's why cadmium removal was affected the most in the presence of NaCl and KCl.
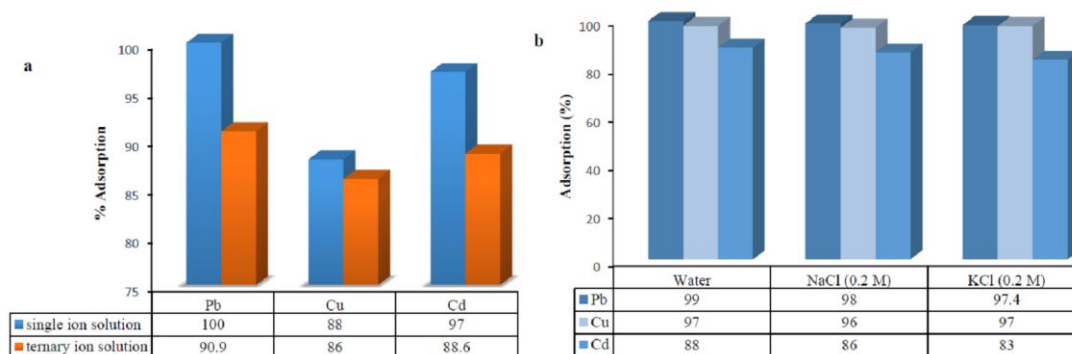

Figure 7. Selectivity of AC-SH, (a) a single and ternary ions solution and (b) electrolyte effect

3.6. Adsorption mechanism

The adsorption mechanism of heavy metals onto AC-SH is complicated and is a combination of electrostatic attraction and chemical interaction between the metal ions and the surface functional groups [19]. Nevertheless, the major adsorption mechanism is due chemical interaction (ions speciation as a function of pH). AC-SH surface contains acidic groups besides the sulfer moieties. Carboxylic acid groups are responsible for the cation exchange capacity of carbon sorbents. Figure 8(a) illustrate the infrared spectra for AC-SH before and after metal ions adsorption. After metal complexing, the band characteristic for thiol group disappeared, which proves the interaction between -SH and metal ions. Also the band characteristic for carboxylic acid decreased significantly. These results verify the interaction of the sulfer groups and acidic groups found on the carbon surface with the metal ions during the adsorption process. A proposed schematic illustration is shown Figure 8(b).
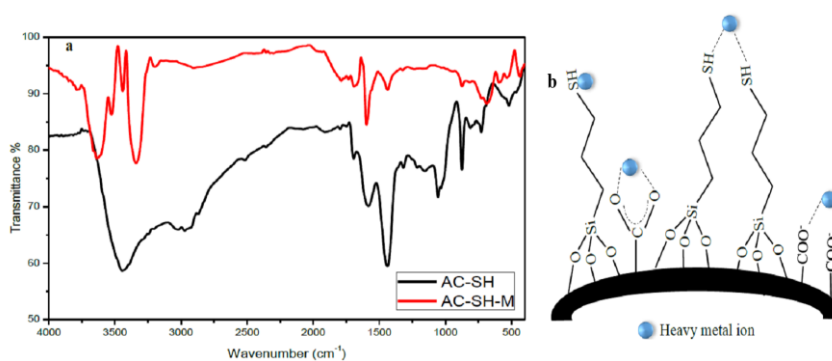

Figure 8. Infrared spectra for AC-SH, (a) before and after metal ions adsorption, (b) a proposed mechanism of adsorption on AC-SH

The maximum adsorption capacities obtained in this study were found to be higher than those reported in the literature as shown in Table 3. This proves the efficiency of thiol modified oak charcoal for heavy metal ions from water.

Table 3. Adsorption capacities of several types of thiol modified adsorbents

Adsorbent	Metal ion	q_{max} (mg g^{-1})	Ref
Silica gel	Cu^{2+}	186	[20]
Nanoporous silica	Hg^{2+}	118	[21]
	Cu^{2+}	89.5	
Spent Grain	Pb^{2+}	20`9	[22]
	Zn^{2+}	227	
	Cd^{2+}	303	
SBA-16	Cu^{2+}	36	[23]
Mesoporous CMK-3 carbon	Pb^{2+}	177	[24]
	Zn^{2+}	29	
	Cu^{2+}	214	
Oak charcoal	Pb^{2+}	250	This study
	Cd^{2+}	197	

4.   CONCLUSION

In this study, oak charcoal was modified with thiol functional groups in order to be utilized as a heavy metals adsorbent. The modified carbon has proved to be effective in eliminating Cd^{2+}, Pb^{2+}, and Cu^{2+} ions from water. The adsorption capacities were 197, 250, and 214 mg g^{-1} for Cd^{2+}, Pb^{2+}, and Cu^{2+} ions respectively. pH had the major effect on the adsorption capacity since it controls metal ions speciation in the solution as well as the surface charge. The process of adsorption obeys the pseudo second order kinetic model for all metal ions. The Freundlich model fitted better for Cu^{2+} and Cd^{2+} while Langmuir model gave a better fit for Pb^{2+}. The adsorbent was selective for Pb^{2+}. A mechanism of adsorption was proposed and it was found that both thiol moieties and carboxylic acid groups are involved in the adsorption process.

REFERENCES

[1]   Hamad H, Ezzeddine Z, Lakis F, Rammal H, Srour M, Hijazi A., "An insight into the removal of Cu (II) and Pb (II) by aminopropylmodified mesoporous carbon CMK-3: Adsorption capacity and mechanism. *Materials Chemistry and Physics*, vol. 178, pp. 57-64, 2016, doi: 10.1016/j.matchemphys.2016.04.062.

[2]   Dumrul H, Kursunlu AN, Kocyigit O, Guler E, Ertul S., "Adsorptive removal of Cu (II) and Ni(II) ions from aqueous media by chemical immobilization of three different aldehydes," *Desalination*, vol. 271, no. 1-3, pp. 92–99, 2011, doi: 10.1016/j.desal.2010.12.017.

[3]   Chingombe P, Saha B, Wakeman RJ, "Surface modification and characterisation of a coal-based activated carbon," *Carbon*, vol. 43, no. 15, pp. 3132-3143, 2005, doi: 10.1016/j.carbon.2005.06.021.

[4]   Hamad H, Ezzeddine Z, Kanaan S, Lakis F, Hijazi A, Moussawi MA., "A novel modification and selective route for the adsorption of Pb^{2+} by oak charcoal functionalized with glutaraldehyde," *Advanced Powder Technology*, vol. 27, no. 2, pp. 631–637, 2016, doi: 10.1016/j.apt.2016.02.019.

[5]   Sato S, Yoshihara K, Moriyama K, Machida M, Tatsumoto H., "Influence of activated carbon surface acidity on adsorption of heavy metal ions and aromatics from aqueous solution," *Applied Surface Science*, vol. 253, no. 20, pp. 8554–8559,2007, doi: 10.1016/j.apsusc.2007.04.025.

[6]   Zhu J, Yang J, Deng B., "Enhanced mercury ion adsorption by amine-modified activated carbon," *Journal of Hazardous Materials*, vol. 166, no. 2-3, pp. 866–872, 2009, doi: 10.1016/j.jhazmat.2008.11.095.

[7]   Macias-Garcia A, Gomez-Serrano V, Alexandre-Franco MF, Valenzuela- Calahorro C, "Adsorption of cadmium by sulphur dioxide treated AC," *Journal of Hazardous Materials*, vol. 103, no. 1-2, pp. 141–152, 2003, doi: 10.1016/s0304-3894(03)00243-7.

[8]   Li YH, Lee CW, Gullett BK., "Importance of AC's oxygen surface functional groups on elemental mercury adsorption," *Fuel,* vol. 82, no. 4, pp. 451–457, 2003, doi: 10.1016/S0016-2361(02)00307-1.

[9]   Domingo-Garcia M, Lopez-Garzon FJ, Perez-Mendoza M., "Effect of some oxidation treatments on the textural characteristics and surface chemical nature of an activated carbon," *Journal of Colloid and Interface Science*, vol. 222, no. 2, pp. 233–240, 2000, doi: 10.1006/jcis.1999.6619.

[10]   Puziya AM, Poddubnaya OI, Zaitsev VN, Konoplitska OP., "Modeling of heavy metal ion binding by phosphoric acid activated carbon," *Applied Surface Science*, vol. 221, no. 1-4, pp. 421–429, 2004, doi: 10.1016/S0169-4332(03)00956-5.

[11]   Hadi M, Samarghandi MR, McKay G., "Equilibrium two-parameter isotherms of acid dyes sorption by activated carbons: study of residual errors," *Chemical Engineerig Journal*, vol. 160, no. 2, pp. 408–416, doi: 10.1016/j.cej.2010.03.016.

[12] Tingaut P, Hauert R, Zimmermann T., "Highly efficient and straightforward functionalization of cellulose films with thiol-ene click chemistry," *Journal of Materials Chemistry*, vol. 21, no. 40, pp. 16066-16076, 2011, doi: 10.1039/C1JM11620G.

[13] McCarthy SA, Davies GL, Gun'ko YK., "Preparation of multifunctional nanoparticles and their assemblies," *Nature Protocols*, vol. 7, no. 9, pp. 1677–1693, 2012, doi: 10.1038/nprot.2012.082.

[14] Aguado J, Arsuaga J, Arencibia A, Lindo M, Gascón V., "Aqueous heavy metals removal by adsorption on amine-functionalized mesoporous silica," *Journal of Hazardous Materials*, vol. 163, no. 1, pp. 213–221, 2009, doi: 10.1016/j.jhazmat.2008.06.080.

[15] Ezzeddine Z, Batonneau-Gener I, Pouilloux Y, Hamad H., "Removal of methylene blue by mesoporous CMK-3: Kinetics, isotherms and thermodynamics," *Journal of Molecular Liquids*, vol. 223, pp. 763–770, 2016, doi: 10.1016/j.molliq.2016.09.003.

[16] Langmuir I., "The constitution and fundamental properties of solids and liquids, Part I. Solids," *Journal of American Chemical Society*, vol. 38, no. 11, pp. 2221–2295, 1916, doi: 10.1021/ja02268a002.

[17] Freundlich HM., "Uber die adsorption in lo sungen," *Journal of Physical Chemistry*, vol. 57, no. 1, pp. 385–471, 1906, doi: 10.1515/zpch-1907-5723.

[18] Kang T, Park Y, Yi J., "Highly selective adsorption of Pt^{2+} and Pd^{2+} using thiolfunctionalized mesoporous silica," *Industrial & Engineering Chemistry Research*, vol. 43, no. 6, pp. 1478–1484, 2004, doi: 10.1021/ie030590k.

[19] Machida M, Fotoohi B, Amamo Y, Ohba T, Kanoh H, Mercier L., "Cadmium (II) adsorption using functional mesoporous silica and activated carbon," *Journal of Hazardous Materials*, vol. 221-222, pp. 220–227, 2012, doi: 10.1016/j.jhazmat.2012.04.039.

[20] Najafi M, Rostamian R, Rafati AA., "Chemically modified silica gel with thiol group as an adsorbent for retention of some toxic soft metal ions from water and industrial effluent," *Chemical Engineering Journal*, vol. 168, no. 1, pp. 426–432, 2011, doi: 10.1016/j.cej.2010.12.064.

[21] Brown J, Mercier L, Pinnavaia TJ., "Selective adsorption of Hg^{2+} by thiolfunctionalized nanoporous silica," *Chemical Communication*, vol. 1, pp. 69–70, 1999, doi: 10.1039/A807249C.

[22] Chai L, Li Q, Zhu Y, Zhang Z, Wang Q, Wang Y, Yang Z., "Synthesis of thiol functionalized spent grain as a novel adsorbent for divalent metal ions," *Bioresource Technology*, vol. 101, no. 15, pp. 6269–6272, 2010, doi: 10.1016/j.biortech.2010.03.009.

[23] Xue X, Li F., "Removal of Cu (II) from aqueous solution by adsorption onto functionalized SBA-16 mesoporous silica," *Microporous and Mesoporous Materials*, vol. 116, no. 1-3, pp. 116–122, 2008, doi: 10.1016/j.micromeso.2008.03.023.

[24] Michalak-Zwierz K, Gdula K, Tyszczuk-Rotko K, Zawadzki W, Dąbrowski A, Barczak M., "Thiol-Functionalized Mesoporous Carbons as Adsorbents of Heavy-Metal Ions," *Adsorption Science & Technology*, vol. 33, no. 6-8, pp. 663–6688, 2015, doi: 10.1260/0263-6174.33.6-8.663.